Dalton Transactions

Accepted Manuscript

ROYAL SOCIETY OF CHEMISTRY

www.rsc.org/dalton

TOC Graphic

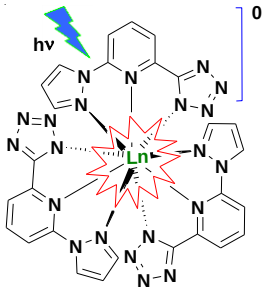

We report the synthesis and efficient photoluminescence of charge-neutral lanthanide (Ln = Eu^{3+} and Tb^{3+}) complexes based on pyrazole-pyridine-tetrazole and pyrazole-pyridine-triazole ligands.

Highly luminescent charge-neutral europium (III) and terbium (III) complexes with tridentate nitrogen ligands†

Kuppusamy Senthil Kumar, [a] Bernhard Schäfer, [b] Sergei Lebedkin, [b] Lydia Karmazin, [c] Manfred M. Kappes[b,d] and Mario Ruben[a,b]*

[a]Institut de Physique et Chimie des Matériaux de Strasbourg (IPCMS), CNRS-Université de Strasbourg, 23, rue du Loess, BP 43, 67034 Strasbourg cedex 2, France.
[b]Institute of Nanotechnology, Karlsruhe Institute of Technology (KIT), Hermann-von-Helmholtz-Platz 1, 76344, Eggenstein-Leopoldshafen, Germany.
[c]Service de Radiocristallographie, Institut de Chimie de Strasbourg UMR7177 CNRS-Université de Strasbourg, 1 rue Blaise Pascal, BP 296/R8, 67008 Strasbourg cedex, France.
[d]Institute of Physical Chemistry, Karlsruhe Institute of Technology (KIT), Fritz-Haber-Weg 2, 76131 Karlsruhe, Germany.
*Email: mario.ruben@kit.edu

†Electronic supplementary information (ESI) available: Synthesis of ligands and their lanthanide complexes, UV-vis, photoluminescence excitation (PLE) and photoluminescence emission (PL) spectra of ligands and lanthanide complexes in solid state and ethanol (EtOH) solvent medium are available. CCDC reference numbers 1057179 and 1057180.

Abstract

We report on the synthesis of tridentate-nitrogen pyrazole-pyridine-tetrazole (L^1H) and pyrazole- pyridine-triazole (L^2H) ligands and their complexation with lanthanides (Ln = Gd(III), Eu(III) and Tb(III)) resulting in stable, charge-neutral complexes $Ln(L^1)_3$ and $Ln(L^2)_3$, respectively. X-ray crystallographic analysis of the complexes with L^1 ligands revealed tricapped trigonal coordination geometry around the lanthanide ions. All complexes show bright photoluminescence (PL) in the solid state, indicating efficient sensitization of the lanthanide emission via the triplet states of the ligands. In particular, the terbium complexes show high PL quantum yields of 65 and 59% for L^1 and L^2, respectively. Lower PL efficiencies of the europium complexes (7.5 and 9%, respectively) are attributed to large energy gaps between the triplet states of the ligands and accepting levels of Eu(III). The triplet state energy can be reduced by introducing an electron withdrawing (EW) group at the 4 position of the pyridine ring. Such substitution of L^1H with a carboxylic ester (COOMe)

EW group leads to an europium complex with increased PL quantum yield of 31%. A comparatively efficient PL of the complexes dissolved in ethanol indicates that the lanthanide ions are shielded against nonradiative deactivation via solvent molecules.

Introduction

Lanthanide complexes are attractive luminophors due to their characteristic, narrow emission lines of different colors. [1] Numerous applications ranging from organic light emitting diodes [2] and optical fibres,[3] to probes for bio imaging[4] and solar energy conversion[5] have been proposed based on the photoluminescence (PL) of lanthanide complexes. Due to their parity forbidden intrashell f-f transitions, the lanthanide ions feature very low absorption coefficients and their direct photoexcitation is inefficient.[6] Therefore, PL of the lanthanides is typically sensitized via energy transfer from excited states of organic ligands with high absorption coefficients in the UV and/or visible spectral regions.[7] The sensitization process usually involves a triplet excited state of a ligand, thus requiring efficient intersystem conversion in the ligand (which may be facilitated by the lanthanide ions) as well as a proper alignment of the triplet state energy (E_T) over that of the accepting lanthanide state(s).[8] An energy gap (ΔE) of ~2,500-3000 cm^{-1} has been argued to be optimal.[9] Lower ΔE values would enable back energy transfer and thus reduce sensitization efficiency. The sensitization and lanthanide emission compete with various non-radiative deactivation processes. The latter prevail in numerous lanthanide complexes, resulting in a poor overall PL quantum yield. Several classes of organic ligands have so far been identified, which can provide for stable and highly luminescent lanthanide complexes.[7,10] In this regard, several pyridyl-pyrazole[11a-f] and pyridyl-tetrazole[11g-h] based ligand systems were developed, in particular, tridentate ligands with mixed N, O or all-nitrogen coordination sites have recently attracted significant attention.[12] For instance, Bünzli and co-workers reported neutral complexes based on benzimidazole-pyridine-tetrazolate ligands, featuring remarkable sensitization efficiency of the europium emission.[13] Nearly 100% PL efficiency was reported for the Tb(III) emission in a bis-tetrazole-pyridine complex.[14] Although PL quenching via solvent (e.g. water) molecules was observed in some of those complexes, this problem appears surmountable and consequently the tridentate all-nitrogen ligands have a big potential for designing lanthanide compounds with a stable and closed inner coordination shell (and, consequently, bright emission in a solution). In addition, they readily allow to position various substituents on the ligand frame, thus opening the possibility to adjust the electronic properties of the ligands for specific lanthanide ions.

In this contribution, we describe the synthesis and photophysical properties of tridentate-nitrogen pyrazole-pyridine-tetrazole (L^1H) and pyrazole-pyridine-triazole (L^2H) ligands and their complexes with lanthanides Gd(III), Eu(III) and Tb(III) (Scheme 1). The Eu(III) and Tb(III) complexes are brightly luminescent. Furthermore, they increase a so far small number of known all nitrogen based *charge-neutral* lanthanide complexes.[13] Charge neutrality can be advantageous or even necessary for a number of applications, including, for instance, assembling molecule-nanostructure hybrid devices in the field of molecular electronics. Such a charge-neutral terbium complex (single molecule magnet) has been successfully coupled to a single-walled carbon nanotube.[15] Luminescent lanthanide complexes anchored to graphene or a nanotube might provide a molecular 'ruler' by making use of a distance-dependent quenching effect - in analogy to lanthanide-quantum dot[16a] and quantum dot-graphene hybrids.[16b-c]

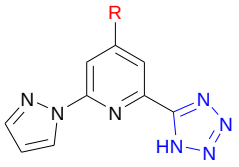

L^1H: R= H
L^1H-COOMe: R=COOMe

$Ln(L^1)_3$:
1. $Gd(L^1)_3$
2. $Eu(L^1)_3$
3. $Tb(L^1)_3$

and

$Ln(L^1\text{-}COOMe)_3$:
4. $Gd(L^1\text{-}COOMe)_3$
5. $Eu(L^1\text{-}COOMe)_3$
6. $Tb(L^1\text{-}COOMe)_3$

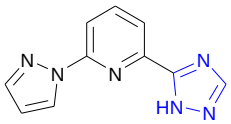

L^2H

$Ln(L^2)_3$:
7. $Gd(L^2)_3$
8. $Eu(L^2)_3$
9. $Tb(L^2)_3$

Scheme 1 Ligands and lanthanide complexes synthesized in this work.

Results

Synthesis

The synthesis of ligand L^1H was carried out starting from 2, 6-dibromopyridine as shown in scheme 2. This improved the overall yield to 78% relative to 37% as reported in our previous study for a reaction starting from 2-bromopyridine.[17] The same synthetic pathway was also utilized to obtain ligand L^1H-COOMe with a carboxylic ester electron-withdrawing group at the 4 position of pyridine ring.

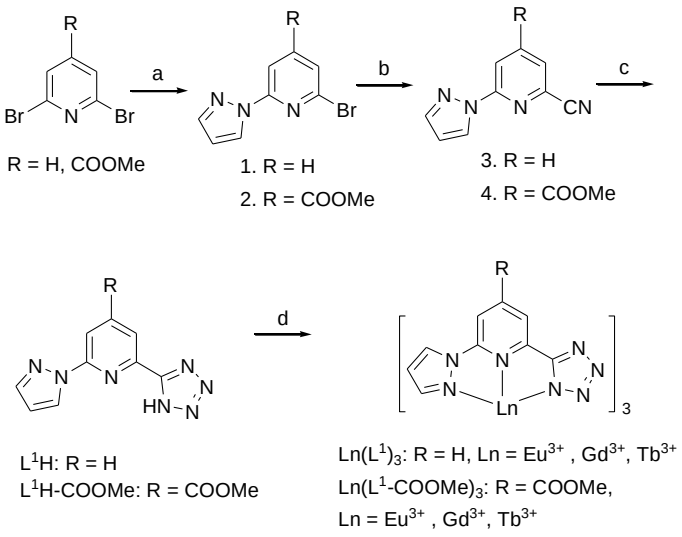

Scheme 2 Synthesis of ligands L^1H and L^1H-COOMe and their Gd, Eu and Tb complexes; reaction conditions: (a) NaH/pyrazole in DMF, 80°C, under Ar, 45 min then 2,6-dibromopyridine or 2,6-dibromoisonicotinic acid methyl ester, 130°C, under Ar, 2 h; (b) CuCN in DMF, 150°C, under Ar, 4 h; (c) NaN_3/NH_4Cl in DMF, 130°C, 20 h; (d) Et_3N, $LnCl_3 \cdot 6H_2O$ (Ln = Eu or Gd or Tb) in DCM/MeOH (7:3), rt, 2 h (see also experimental section).

The ligand L^2H was obtained from compound **3** depicted in scheme 2. Its reaction with hydrazine hydrate in ethanol yielded picolinohydrazonamide (scheme 3).

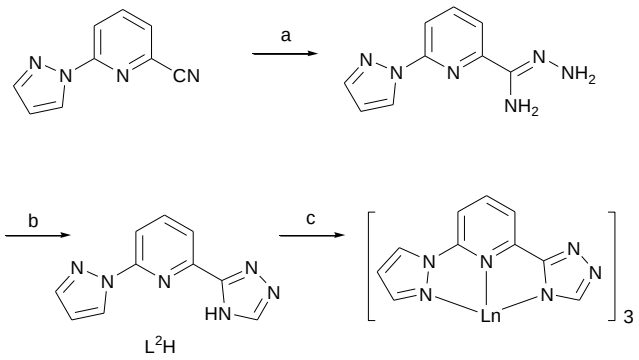

Scheme 3 Synthesis of L^2H and its lanthanide complexes; Reaction conditions: (a) $NH_2NH_2 \cdot H_2O$ in EtOH, rt.; (b) HCOOH, 9°C (0.5 h.), 100°C (18 h.); (c) aqueous NaOH (base) $LnCl_3 \cdot nH_2O$ in H_2O, EtOH or MeOH, in air.

The latter was reacted with formic acid to produce the expected ligand L^2H in a moderate yield after purification by column chromatography. The charge-neutral lanthanide complexes

(Ln = Gd, Eu and Tb) were prepared with the aforementioned ligands as depicted in schemes 2 and 3.

Crystallographic analysis

Single crystals of the complexes **2** and **3** (see scheme 1) suitable for X-ray structural analysis were obtained after complexation in a dilute solution with the ligand and $LnCl_3 \cdot 6H_2O$ in a 3·8:1 ratio. Slow evaporation of the reaction mixture over 1-2 weeks under ambient conditions yielded X-ray quality crystals. Our efforts to crystallize other complexes with L^1H-COOMe and L^2H ligands have so far been unsuccessful (resulting in polycrystalline products).

The isostructural complexes **2** and **3** crystallized in a trigonal crystal system with R-3 space group. A coordination number of nine was obtained with three nitrogen atoms from each ligand donating electron density to the lanthanide ion as shown in Fig. 1a and b for the complex **2**.

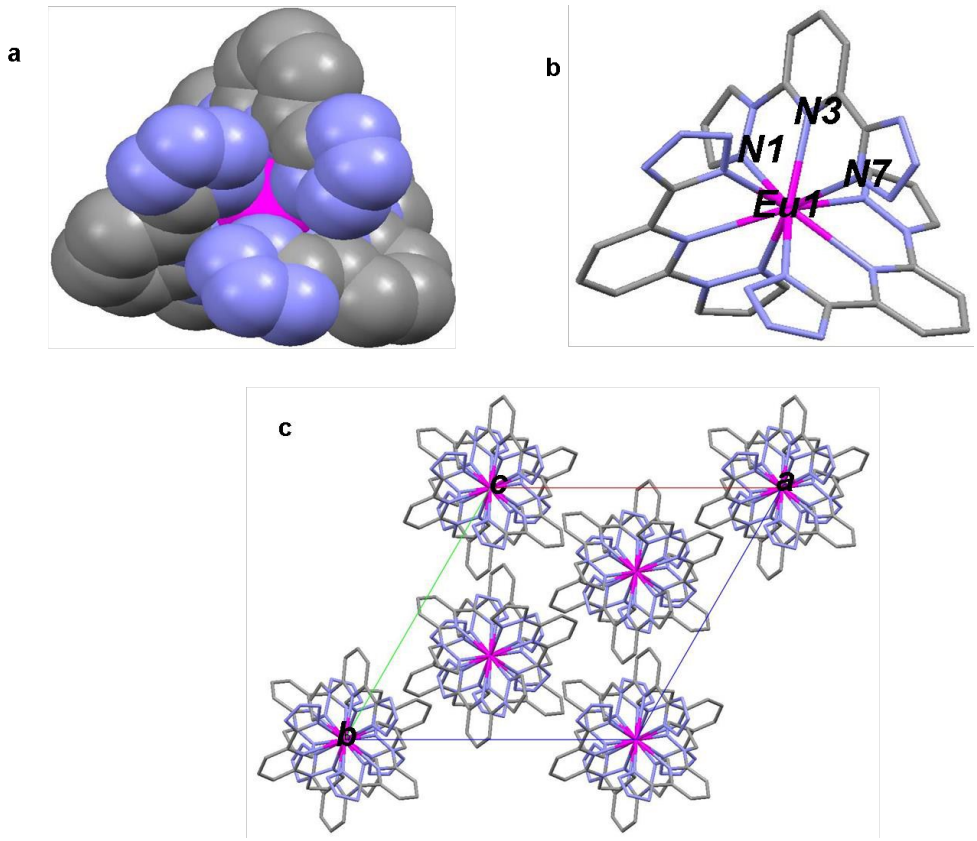

Fig. 1 (a) Space filling representation and **(b)** stick diagram of complex **2** showing helical arrangement of three tridentate L^{1-} ligands around the central Eu(III) ion as viewed down

crystallographic c axis (H atoms and solvent molecules are omitted for clarity). (**c**) Unit cell packing pattern viewed down crystallographic c axis.

Each complex molecule is surrounded by three methanol solvent molecules which are hydrogen bonded to the Ln-noncoordinated tetrazole nitrogen of the ligand. The coordination environment around the lanthanide ion can be described as tricapped trigonal prism with three ligand molecules arranged in a helical fashion as in the case of previously reported tetrazole based system, both Δ and Λ enantiomers are present in the overall racemic crystal lattice (Fig. 1c).[12b] The values of the Eu-N bond lengths are 2.556(2), 2.618(2) and 2.512(2) Å for Eu-pyrazole (Eu1-N1), Eu-pyridine (Eu1-N3) and Eu-tetrazole (Eu1-N7) bonds respectively (Fig. 1b). Bite angles of 61.57(5)° and 63.71(5)° are observed for the N1(pyrazole)-Eu1-N3(pyridine) and N7(tetrazole)-Eu1-N3(pyridine) coordinating units. Overall, obtained bond lengths and angles are in line with the previously reported values for similar tetrazole- and pyrazole-based lanthanide complexes.[11g,18] Further details of the crystal structures are depicted in table 1. In the text, for simplicity, the composition of solid complexes is noted without solvent molecules.

Table 1 Crystallographic data of the Lanthanide complexes **2** and **3**

Complex	$Eu(L^1)_3.3MeOH$ (**2**)	$Tb(L^1)_3.3MeOH$ (**3**)
Formula	$C_{30}H_{30}EuN_{21}O_3$	$C_{30}H_{30}N_{21}O_3Tb$
FW/g.mol^{-1}	884.71	891.67
T/K	173	173
Crystal System	Trigonal	Trigonal
Space group	R-3	R-3
a/Å	16.997(5)	16.980(5)
b/Å	16.997(5)	16.980(5)
c/Å	21.834(5)	21.806(5)
α/°	90	90
β/°	90	90
γ/°	120	120
V/Å^3	5463(3)	5445(3)
Z	6	6
ρ/g.cm^{-3}	1.614	1.632

μ/mm^{-1}	1.787	2.014
θ min-max/°	1.668, 31.005	1.670, 31.031
Reflns. collected	14715	14660
Indep. Reflns.	3878	3871
Parameters	168	168
GOF on F^2	1.049	1.078
R1, wR2	0.0276, 0.0604	0.0228, 0.0510
R1, wR2 (all data)	0.0364, 0.0622	0.0274, 0.0519

Photophysical properties of ligands and complexes

Electronic absorption characteristics of ligands and complexes

Due to poor solubility of the complexes in common organic solvents, UV-vis absorption spectra of the ligands and complexes were measured in dimethylsulfoxide (DMSO) immediately after dissolution. The complexes were found to be stable in this solvent, at least within few hours of solubilisation as inferred from the UV-vis measurements as well as from NMR measurement of the complex 5 in deuterated DMSO wherein identical spectra were observed for the sample measured at t = 0 and 1h (Figure S1). Fig. 2a-c shows the normalized spectra of the ligands and corresponding Eu and Tb complexes. In general, the absorption maxima of the complexes are slightly bathochromically shifted in comparison to the ligand compounds.

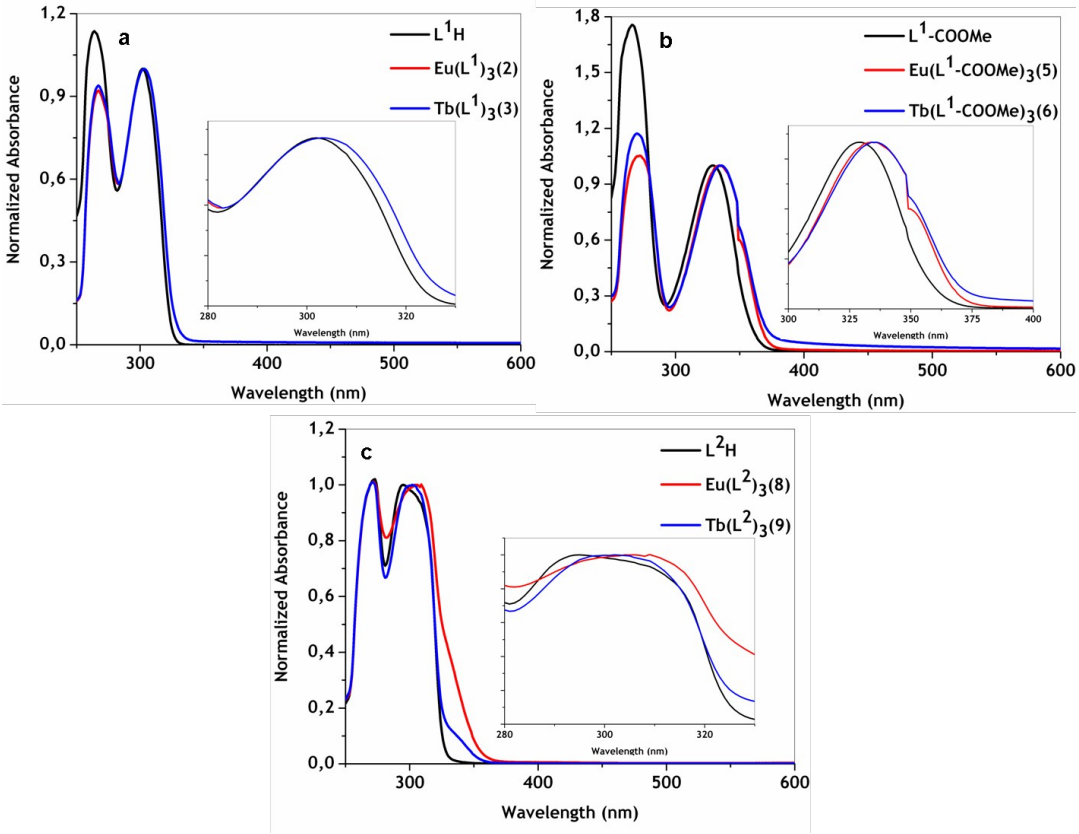

Fig. 2(a-c) UV-vis absorption spectra of the ligands and Eu(III) and Tb(III) complexes in DMSO at 295K, spectra are normalized at the lowest absorption maxima, insets show the expanded part of the spectra around the lowest absorption maxima.

A more pronounced bathochromic shift of the absorption is observed for the L^1H-COOMe ligand and its lanthanide complexes (onset of absorption at ~370 nm) in comparison to the parent L^1H ligand and its complexes (at ~325 nm). It can be attributed to a lowering of the HOMO-LUMO gap due to the presence of COOMe electron withdrawing group at the 4th position of the pyridine ring. The red-shift of the absorption edge up to ~370 nm, *i.e.* closer to the visible region, simplifies selection of an excitation light source and thus can be beneficial for applications. Note that the lanthanide complexes show higher molar absorptivity coefficients in comparison to the ligands (table 2) due to the presence of three coordinated ligands.

Table 2 Absorption maxima (λ_{max}) and molar absorptivity coefficients (ε) of ligands and complexes measured in DMSO solution at 295 K and triplet state ($^3\pi\pi^*$) energies of ligands as

determined from photoluminescence maxima measured at 20K in solid gadolinium complexes.

Molecule	λ_{max}/nm ($\varepsilon/10^{-4}$ cm^{-1} M^{-1})	$^3\pi\pi^*/cm^{-1}$
L^1H	264 (1.3), 302 (1.2)	23900
$Eu(L^1)_3$ (**2**)	267 (2.9), 302 (3.2)	
$Tb(L1)_3$ (**3**)	267 (3.0), 302 (3.2)	
L^1H-COOMe	267 (2.1), 329 (1.2)	23000
$Eu(L^1\text{-COOMe})_3$ (**5**)	272 (2.7), 334 (2.5)	
$Tb(L^1\text{-COOMe})_3$ (**6**)	271 (2.6), 335 (2.2)	
L^2H	272 (0.91), 294 (0.91)	22700
$Eu(L^2)_3$ (**8**)	272 (2.6), 305 (2.6)	
$Tb(L^2)_3$ (**9**)	271 (2.7), 303 (2.6)	

Photoluminescence of ligands.

The ligands show bright fluorescence in the solid state, which peaks at 365, 375 and 348 nm for L^1H (Fig. 3a), L^1H-COOMe (Fig. 3b) and L^2H (Fig. 3c), respectively. The phosphorescence of the ligand compounds is apparently very weak, also at cryogenic temperatures, and could not be detected on our apparatus (without time-discrimination option). To estimate triplet energies of the ligands, E_T, in the lanthanide complexes, the ligand-based phosphorescence spectra were measured for the gadolinium complexes (demonstrating no lanthanide-centred emission).

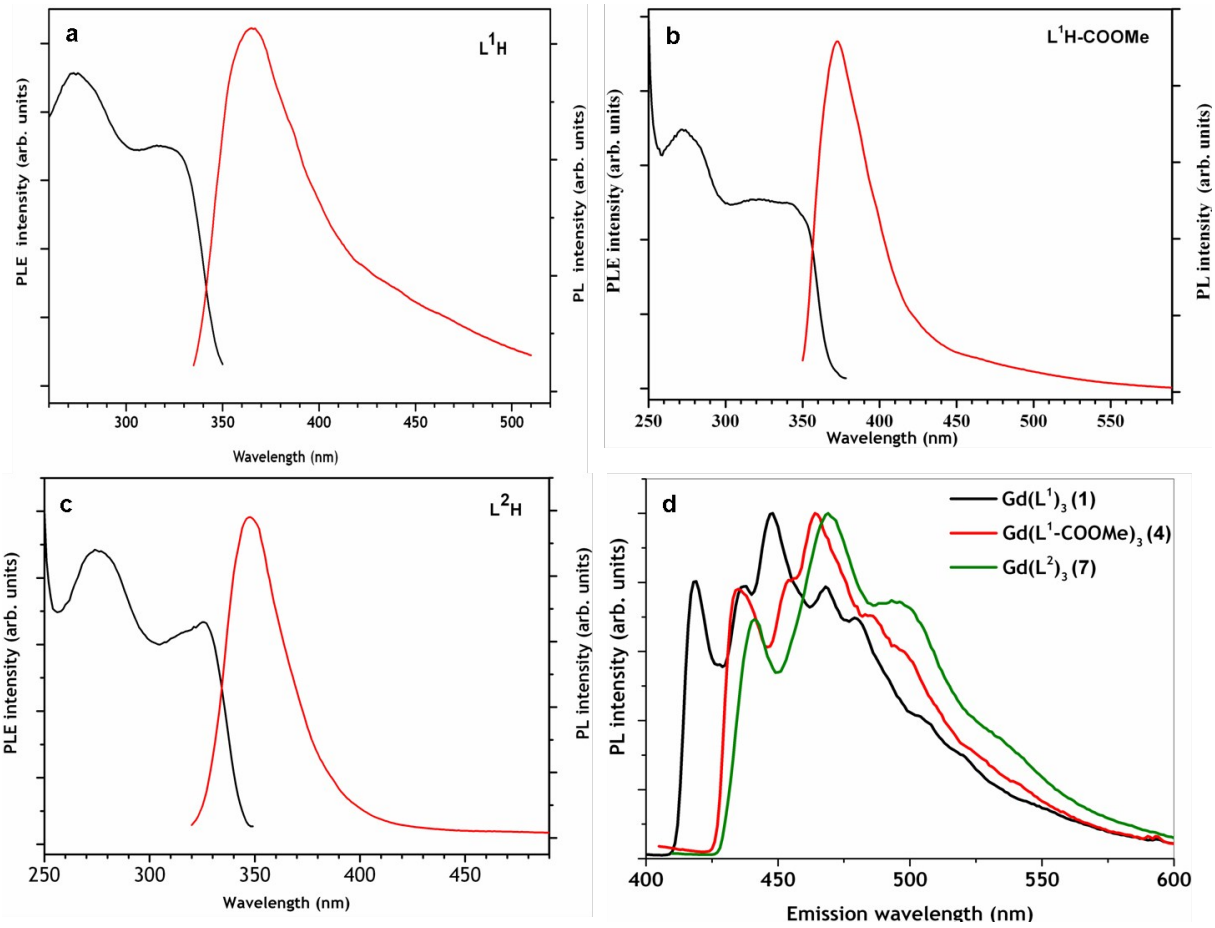

Fig. 3(a-c) PLE and PL spectra of ligands at 295 K in solid state, the PL and PLE spectra were excited and recorded at 300 and 370 nm for L^1H and L^1H-COOMe and 300 and 360 nm for L^2H respectively. **(d)** Ligand-centred phosphorescence spectra of solid Gd complexes measured at 20K.

Only very weak ligand fluorescence at ambient temperature, but bright ligand-centred phosphorescence at temperatures below ~100 K was observed for the latter (Fig. 3d). This indicates an efficient intersystem conversion in the ligands caused by the presence of the Gd ions. The values of E_T estimated from the 0-0 transitions are listed in table 2. The triplet state of L^1H-COOMe was found to be 930 cm^{-1} lower than that of L^1, as attributed to the effect of COOMe electron withdrawing group in L^1H-COOMe.

Photoluminescence of Eu(III) and Tb(III) complexes.

Under photoexcitation into the ligand absorption bands, the solid europium complexes emit characteristic red PL attributed to the $^5D_0 \rightarrow ^7F_j$ (j=1-4) transitions of the Eu(III) ions as shown in Fig. 4a for complex **2** and in Fig. S2b and S3b for complexes **5** and **8,** respectively. The spectra are mainly contributed by the dominating hypersensitive $^5D_0 \rightarrow ^7F_2$ transition as well

as relatively strong $^5D_0 \rightarrow ^7F_1$ and $^5D_0 \rightarrow ^7F_4$ transitions (cf. Fig. 4a). The ligand-based fluorescence is practically absent. The PL excitation (PLE) spectra correspond to the ligand absorption, further indicating the sensitized character of the europium emission.

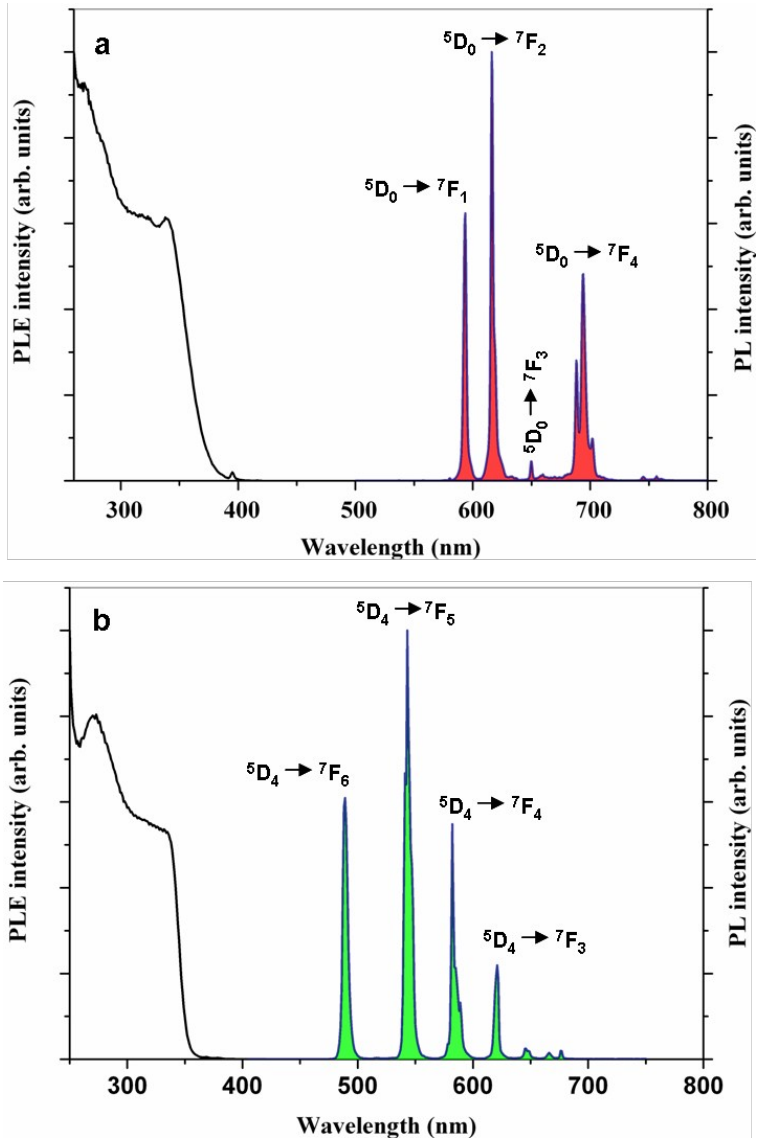

Fig. 4 (a) PLE and PL spectra of solid complex **2** at 295 K, the PL and PLE spectra were excited and recorded at 330 and 617 nm respectively. **(b)** PLE and PL spectra of solid complex **3** at 295 K, the PL and PLE spectra were excited and recorded at 330 and 490 nm.

Table 3 Photophysical parameters of the europium and terbium complexes in the solid state at ambient temperature.

Complex	$\Delta E/cm^{-1}$ [a]	τ_{obs}/ms [b,c]	τ_{rad}/ms [d]	$Q_{Ln}/\%$ [d]	$\eta_{sens}/\%$ [d]	$Q_{tot(solid)}/\%$ [e]	$Q_{tot(Ethanol)}/\%$ [f]
$Eu(L^1)_3$ (**2**)	6690	1.76	4.41	39.9	18.8	7.5	12
$Tb(L1)_3$ (**3**)	3430	1.23				65	19
$Eu(L^1\text{-}COOMe)_3$ (**5**)	5760	2.1	4.5	46.7	66.4	31	19
$Tb(L^1\text{-}COOMe)_3$ (**6**)	2190	1.0				53	14
$Eu(L^2)_3$ (**8**)	5450	1.91	4.47	42.8	21.0	9	12
$Tb(L^2)_3$ (**9**)	2500	1.57				59	23

[a] Energy difference between ligand $^3\pi\pi^*$ and receiving states, [b] after pulsed laser excitation at 337 nm, [c] Estimated error for lifetimes is ±1% , [d] values are not calculated for Tb as it has no isolated MD transition (see ref.6), [e] quantum yields were estimated to be ±10% and [f] quantum yields were estimated to be ±5%.

It is possible to extract structural information such as coordination strength of the ligand and local symmetry from the PL spectra; a relatively low intensity ratio of ~1.6 of the $^5D_0 \rightarrow {}^7F_2$ vs. $^5D_0 \rightarrow {}^7F_1$ transitions indicates a symmetric coordination around the europium ions - in line with the X-ray structure of complex **2**.[6] Under pulsed laser excitation at 337 nm, the PL decays monoexponentially with time constants, τ_{obs}, between 1.76 msec (**2**) and 2.1 msec (**5**) (table 3).[19] These values are similar to those of other brightly luminescent europium complexes.[12] The monoexponential decay indicates the presence of one emissive europium species. The total PL quantum yield, Q_{tot}, can be represented as the product of the sensitization efficiency, η_{sens}, and the intrinsic quantum yield, Q_{Eu}, of the europium emission from the $^5D_0$ level:

$$Q_{tot} = \eta_{sens} \times Q_{Eu} = \eta_{sens} \times (\tau_{obs}/\tau_{rad}) \qquad (1)$$

where τ_{rad} is the radiative lifetime (τ_{rad}) of the $^5D_0$ level. It can be expressed as

$$\tau_{rad} = A_{MD} \times (n)^3 \times I_{tot}/I_{MD} \qquad (2)$$

where, A_{MD} is the spontaneous emission probability for the $^5D_0 \rightarrow {}^7F_1$ transition in vacuum (taken here as 14.65 s^{-1}), n is the refractive index of the solid complex (taken here as 1.5) and I_{tot}/I_{MD} is the ratio of the total integrated emission intensity (for all transitions from the $^5D_0$ state to the ^7F_J manifold (I_{tot})) to that of the magnetic dipole $^5D_0 \rightarrow {}^7F_1$ transition (I_{MD}). The

values of Q_{Eu}, τ_{rad} and η_{sens} calculated from Eqs. 1 and 2 are listed in table 3. The intrinsic Eu quantum yield, Q_{Eu}, of ~40% is similar for all complexes, indicating similar coordination environment of the europium ions. Since the triplet energies, E_T, of the ligands are relatively high (table 2), three Eu(III) levels - ^5D_J , J = 0-2, at about 17230, 19000 and 21600 cm^{-1}, respectively, - can be involved in energy transfer. The total sensitization (energy transfer) efficiency, η_{sens}, may strongly depend on the relative energies of the donor and acceptor states. It increases from ~19% for **2** (E_T = 23900 cm^{-1}) to ~66% for **5** (E_T = 23000 cm^{-1}). The increase of η_{sens} is probably due to the lower energy gaps and more efficient energy transfer to ^5D_J, J = 0, 1 levels in **4** vs. **1**. On the other hand, the sensitization appears to be also sensitive to the ligand structure: **5** and **8** have close-lying energies of the ligand triplets (23000 vs. 22700 cm^{-1}), but distinct values of η_{sens} (66 vs. 21%). The Eu complexes also show bright PL in ethanol solutions (table 3). This indicates a stable coordination and a good shielding of the europium ions against solvent molecules. Some differences in Q_{tot} between the dissolved and solid complexes can be attributed to slight changes in the coordination environment of the europium ions as well as to vibronic quenching of the excited states by OH vibration of EtOH solvent.[20]

The solid terbium complexes show bright green photoluminescence contributed by the characteristic Tb(III) $^5D_4 \rightarrow {}^5F_j$, J = 3-6, transitions between 475 and 650 nm (Fig. 4b, S2C and S3C). The high PL quantum yields of 53-65% are likely facilitated by a good energy match between the donor (triplet ligand) and acceptor ($^5D_4$ at ~20500 cm^{-1}) states (ΔE ~ 2200-3400 cm^{-1}, see table 2). The PL of the terbium complexes decays monoexponentially on the time scale of a few milliseconds (table 3), thus indicating the presence of a single emissive species as in the case of the europium complexes. Similarly, no ligand-based fluorescence or (low-temperature) phosphorescence was detected. In difference to the europium complexes, the PL efficiency of the terbium counterparts reduces more significantly in ethanol solutions as compared to the solid state (table 3). This might be tentatively attributed to some lowering of the ligand triplet state relative to the $^5D_4$ level of Tb(III) which facilitates back energy transfer,[8, 9] as well as to the quenching effect of the solvent (ethanol) molecules[20] as described in the case of Eu complexes.

Discussion

From the above results, the overall PL efficiency of solid complexes can be ordered, depending on the ligand, as L^1H-COOMe >L^2H >L^1H for Eu(III) and L^1H>L^2H >L^1H-

COOMe for Tb(III). Introduction of the COOMe group at the 4th position of the pyridine ring lowers both the singlet and triplet ($^1\pi\pi^*$ and $^3\pi\pi^*$) energies of the L^1H ligand. Such lowering can be attributed to increased conjugation in L^1H-COOMe due to the electron withdrawing nature of the COOMe group. As a result, the singlet energy is shifted to a more convenient excitation spectral range ($^1\pi\pi^*$) whereas the triplet state energy shift allows more efficient energy transfer from the ligand ($^3\pi\pi^*$) to lanthanide ions. Indeed, the introduction of the COOMe group lowers the triplet energy, E_T, from 23900 cm^{-1} (L^1H-complex **2**) to 23000 cm^{-1} (L^1H-COOMe complex **5**), accompanied by an increase of the total PL efficiency, Q_{tot}, from 7.5% to 31%, respectively. Note, however, that the correlation between Q_{tot} and $^3\pi\pi^*$ energy is not as simple as it seems, since as many as three accepting levels of the Eu(III) ions can be involved in the energy transfer (see Results).[9a] Upon moving from Eu to Tb: the COOMe substitution only moderately lowers the Tb quantum yield to 53% for complex **6** (65% for complex **3**). This is probably due to the closer energetic proximity of the $^3\pi\pi^*$ state with respect to the accepting $^5D_4$ level of Tb(III) in complex **6**, thus facilitating back energy transfer. Upon modification of the coordinating ligand from tetrazole (L^1H) to triazole (L^2H) the energies of $^1\pi\pi^*$ and $^3\pi\pi^*$ excited states are lowered, indicating a better π electron donating nature of triazole as compared to tetrazole. However, comparable Eu(III) and Tb(III) luminescence quantum yields (table 3) were found for the L^1H and L^2H systems.

Mazzanti and co-workers have reported efficient sensitization of Eu(III) and Tb(III) luminescence by similar bis-tetrazole-pyridine (H2pytz) and tetrazole-pyridine-carboxylic acid (H2pytzc) ligand systems and proposed the H2pytz based system as a viable alternative to classical dipicolinate (dpa) based systems.[12b] On a comparative scale, the present L^1H and L^2H based ligand systems sensitize Tb(III) luminescence with a similar total efficiency as do H2pytz and H2pytzc ligands, whereas somewhat lower values were obtained for the Eu(III) complexes.

Bünzli and co-workers have recently reported the benzimidazole-pyridine-tetrazolate (bepytet) ligand system with a very high, nearly 100%, Eu(III)-sensitization efficiency.[13] The overall PL efficiency of the solid complexes was, however, reduced in several cases due to the presence of coordinated water molecules. The latter result from a relatively labile coordination by the benzimidazole moiety, leading to an equilibrium between $(Ln(\kappa^3\text{-ligand})_3$ and $(Ln(\kappa^3\text{-ligand})_2(\kappa^1\text{-ligand})\cdot xH_2O$ complexes.[13] In contrast to bepytet, the L^1H ligand studied in this work features a pyrazole moiety instead of benzimidazole. This structural

difference leads to a remarkable 3200 cm^{-1} increase in the $^3\pi\pi^*$ energy in the case of L^1H in comparison with bepytet (E_T = 20700 cm^{-1}). Correspondingly, the bepytet ligand provides for a ~3500 cm^{-1} gap between $^3\pi\pi^*$ energy level and the $^5D_0$ accepting state of Eu(III) and thus appears to be especially suited for europium sensitization. In comparison, the L^1H and L^2H ligands with the higher triplet state energies apparently provide for the more efficient Tb(III) sensitization (Table 3).

Conclusions

Two new families of stable, charge-neutral Eu and Tb complexes have been designed and synthesized based on pyrazole-pyridine-tetrazole (L^1H) and pyrazole-pyridine-triazole (L^2H) ligands. Crystal structures determined for $Eu(L^1)_3$ and $Tb(L^1)_3$ demonstrate tricapped trigonal coordination geometry around the lanthanide ions. The above ligands - similar to other all-nitrogen tridentate ligands reported previously – provide for efficient photosensitization of lanthanide emission. In particular, the Tb complexes show bright PL with overall quantum yields as high as 65% in the solid state at ambient temperature and 23% in ethanol solution. In addition, the ligands allow for versatile chemical modification in order to 'adjust' their electronic properties for specific lanthanide ions. Thus, the introduction of a COOMe electron-withdrawing group into the pyridine moiety of L^1H ligand enhanced the PL efficiency of the solid europium complex from 7.5 to 31%. In ongoing work, we plan to apply the charge-neutral lanthanide complexes for hybrid optoelectronic devices with carbon nanostructures and for the fabrication of solar cells based on luminescence down-shifting associated with lanthanide complexes.[5c]Furthermore, the described tridentate ligands may be probed as selective agents for separation of lanthanides and actinides.[13, 21]

Experimental Section

Materials and methods

Anhydrous DMF, 2, 6-dibromopyridine, pyrazole, cuprous cyanide, sodium azide $EuCl_3 \cdot 6H_2O$, $TbCl_3 \cdot 6H_2O$ and $GdCl_3 \cdot 6H_2O$ were purchased from commercial sources and used as received. The required amount of DMF was removed under positive pressure of Ar while performing reactions under anhydrous conditions. At IPCMS ^1H and ^{13}C NMR spectra were measured with a Bruker Avance 300 spectrometer at 300 and 75 MHZ respectively. Solvent signals were used as references for chemical shift values reported in ppm. At KIT, ^1H and ^{13}C NMR spectroscopic data were recorded on a Bruker Ultrashield plus 500

spectrometer with solvent-proton as internal standard. Electrospray ionization time of flight (ESI TOF) mass spectrometric data were acquired on a micrOTOF-Q II Bruker spectrometer.

Instrumentation

X-ray crystallography: Single crystals of $[Eu(L^1)_3 \cdot 3MeOH]$ and $[Tb(L^1)_3 \cdot 3MeOH]$ were grown by slow evaporation of a CH_2Cl_2/MeOH solution at room temperature. The crystals were placed in oil, and a colourless prism single crystal was selected, mounted on a glass fibre and placed in a low-temperature N_2 gas stream.

X-Ray diffraction data collection was carried out on a Bruker APEX II DUO Kappa-CCD diffractometer equipped with an Oxford Cryosystem liquid N_2 device, using Mo-Kα radiation (λ = 0.71073 Å). The crystal-detector distance was 38mm. The cell parameters were determined (APEX2 software)[22] from reflections taken from tree sets of 12 frames, each at 10s exposure. The structure was solved by direct methods using the program SHELXS-2013.[23] The refinement and all further calculations were carried out using SHELXL-2013.[24] The H-atoms were included in calculated positions and treated as riding atoms using SHELXL default parameters. The non-H atoms were refined anisotropically, using weighted full-matrix least-squares on F^2. A semi-empirical absorption correction was applied using SADABS in APEX2;[22] transmission factors: T_{min}/T_{max} = 0.6712/0.7462. The SQUEEZE instruction in PLATON[25] was applied. The residual electron density was assigned to third a molecule of methanol.

Photophysical measurements: Photoluminescence (PL) measurements were performed on a Horiba JobinYvon Fluorolog-322 spectrometer equipped with a closed-cycle optical cryostat (Leybold) operating at ~20-300 K. Solid samples (crystalline powders) were dispersed in a thin layer of polyfluoroester oil (ABCR GmbH) between two 1 mm quartz plates and mounted on the cold finger of the cryostat. Emission spectra were corrected for the wavelength-dependent response of the spectrometer and detector (in relative photon flux units). Emission decay traces were recorded by connecting a photomultiplier to an oscilloscope (typically via a 500 Ohm load) and using a nitrogen laser for pulsed excitation at 337 nm (~2 ns, ~5 μJ per pulse). Estimated error for lifetimes is ±1%. PL quantum yields (PLQY) of solid samples at ambient temperature were determined according to the method of de Mello et al.,[26] a 10 cm integrating sphere, which was installed into the sample chamber of

the spectrometer. Solution phase PL measurements were performed on a Photon Technology International (PTI) spectrometer at ambient temperature. Ethanol solutions were freshly prepared by stirring for 30 min. a small amount of a complex in 10 ml of ethanol, followed by filtration through a 0.45 μm syringe filter. The final solutions had optical densities around 0.2. Relative quantum yields were measured using $Cs_3((Eu(dpa)_3)$ and $Cs_3((Tb(dpa)_3)$ in 0.1 M Tris buffer (pH = 7.45) as standards for Eu and Tb complexes according to literature procedure.[27-29] The accuracy of the determination of quantum yields was estimated to be ±10% and ±5% for the solid state and solution, respectively.

Acknowledgements

Financial support of the Agence Nationale de la Recherche-Labex NIE 11-LABX-0058_NIE within the investissement d'Avenir program ANR-10-IDEX-0002-02 is greatly acknowledged. MR, MK and SL also acknowledge financial support by the DFG funded Collaborative Research Center TRR 88 ("3MET"). The work carried out at KIT benefitted from equipment infrastructure funded by the Helmholtz Program (STN).

References:

1. (a) D. Parker, *Coord. Chem. Rev.*, 2000, **205,** 109–130; J-C. G. Bünzli, *Chem. Rev.*, 2010, **110,** 2729–2755; (b) S. V. Eliseeva and J. -C. G. Bünzli, *Chem. Soc. Rev.*, 2010, **39,** 189–227; (c) J-C. G. Bünzli and C. Piguet, *Chem. Soc. Rev.*, 2005, **34,** 1048–1077; (d) L. D. Carlos, R. A. S. Ferreira, V. D. Bermudez and S. J. L. Ribeiro, *Adv. Mater.*, 2009, **21,** 509–534; (a) K. Binnemans, *Chem. Rev.*, 2009, **109,** 4283–4374; (e) A. de Bettencourt-Dias, *Dalton Trans.*, 2007, 2229–2241; (f) S. V. Eliseeva and J-C. G. Bünzli, New J. Chem., 2011, **35,** 1165–1176.

2. (a) J. Kido, H. Hayase, K. Hongawa1, K. Nagai and K. Okuyama, *Appl. Phys. Lett.* 1994, **65 (17),** 2124-2126; (b) Y. Cui, B. Chen and G. Qian, *Coord. Chem. Rev.*, 2014, **273–274,** 76–86; (c) M.A. Katkova, *Dalton Trans.*, 2010, **39,** 6599–6612.

3. Kuriki, Y. Koike and Y. Okamoto, *Chem. Rev.*, 2002, **102,** 2347−2356.

4. (a) F. S. Richardson, *Chem. Rev.*, 1982, **82,** 541−552; (b) A. J. Palmer, S. H. Ford, S. J. Butler, T. J. Hawkins, P. J. Hussey, R. Pal, J. W. Walton and D. Parker, *RSC Adv.*, 2014, **4,** 9356-9366; (c) Q. Liu, W. Feng and F. Li, Coord. *Chem. Rev.*, 2014, **273–274,** 100–110; (d) D. Tu, W. Zheng, Y. Liu, H. Zhu and X. Chen, *Coord. Chem. Rev.*, 2014, **273–274** 13–29; (e) A. Picot, A. D'Aléo, P. L. Baldeck, A.Grichine, A. Duperray, C. Andraud and O. Maury, *J.*

Am. Chem. Soc., 2008, **130 (5)**, 1532–1533; (f) A. J. Amoroso and S. J. A. Pope, *Chem. Soc. Rev.*, 2015, **44,** 4723-4742.

5. (a) J-C. G. Bünzli and S.V. Eliseeva, *J. Rare Earths*, 2012, **28,** 824; (b) J.-C. G. Bünzli and A.-S. Chauvin, Handbook on the Physics and Chemistry of Rare Earths; J.-C. G. Bünzli and V. K. Pecharski, Eds.; Elsevier Science Publishers: Amsterdam, 2014; **Vol. 44,** Chapter 261, pp 169−281; (c) X. Huang, S. Han, W. Huang and X. Liu, *Chem. Soc. Rev.*, 2013, **42,** 173-201.

6. J-C. G. Bünzli and S. V. Eliseeva, Lanthanide Luminescence: Photophysical, Analytical and Biological Aspects, Springer Series on Fluorescence, P. Hänninen and H. Härmä (Eds.), Springer, 2011.**Vol. 7**, Chapter 1, pp 1-46.

7. J-C. G. Bünzli, *Coord. Chem. Rev.*, 2015, **293-294,** 19-47.

8. (a) A. de Bettencourt-Dias, P. S. Barber and S. Viswanathan, *Coord. Chem. Rev.*, 2014, **273-274**, 165-200; (b) G. F. de Sa´, O. L. Malta, C. de Mello Donega´, A.M. Simas, R.L. Longo, P.A. Santa-Cruz and E.F. da Silva Jr, *Coord. Chem. Rev.*, 2000, **196**, 165–195; (c) S. Sato and M. Kleinerman, *J. Chem. Phys.*, 1969, **51,** 2370−2381; (d) Y. Matsuda, S. Makishima and S. Shionoya, *Bull. Chem. Soc., Jpn.* 1968, **41,** 1513−1518; (e) S. I. Weissman, *J. Chem. Phys.*, 1942,**10,**214.

9. (a) M. Latva, H. Takalo, V. M. Mukkala, C. Matachescu, J. C. Rodriguez-Ubis and J. Kankare, *J. Lumin.*, 1997, **75,** 149−169; (b) M. Wada, *Bull. Chem. Soc. Jpn.*, 1970, **43,** 1955−1962.

10. (a) M. Starck, P. Kadjane, E. Bois, B. Darbouret, A. Incamps, R. Ziessel and L. J. Charbonnière, *Chem. Eur. J.*, 2011, **17,** 9164–9179; (b) E. Brunet, O. Juanes, R. Sedano and J.-C. Rodriguez-Ubis, *Photochem. Photobiol. Sci.*, 2002, **1,** 613–618.

11. (a) E. Brunet, O. Juanes, R. Sedano and J-C. Rodriguez -Ubis, *Org. Lett.*, 2002, **4,** 213-216; (b) M. J. Remuinan, H. Roman, M. T. Alonso and J-C. Rodriguez-Ubis, *J. Chem. Soc. Perkin Trans., 2,* 1993, 1099-1102 ; (c) E. Brunet, O. Juanes, R. Sedano and J-C. Rodriguez -Ubis, *Tetahedron Lett.*, 2007, **48,** 1091–1094 ; (d) E. Brunet, O. Juanes, R. Sedano and J-C. Rodriguez -Ubis, *Tetrahedron*, 2005, **61,** 6757–6763 ; (e) C. P. Montgomery, D. Parker and L. Lamarque, *Chem. Commun.*, 2007, 3841–3843; (f) C. P. Montgomery, E. J. New, L. O.

Palsson, D. Parker, A. S. Batsanov and L. Lamarque, *Helv. Chim. Acta*, 2009, **92,** 2186-2213; (g) M. Giraud, E. S. Andreiadis, A. S. Fisyuk, R. Demadrille, J. Pécaut, D. Imbert and M. Mazzanti, *Inorg. Chem.*, 2008, **47,** 3952– 3954; (h) E. S. Andreiadis, R. Demadrille, D. Imbert, J. Pécaut and M. Mazzanti, *Chem. Eur. J.*, 2009, **15,** 9458– 9476.

12. (a) G. Bozoklu, C. Marchal, J. Pécaut, D. Imbert and D. Mazzanti, *Dalton Trans.*, 2010, **39,** 9112–9122; (b) E. S. Andreiadis, D. Imbert, J. Pécaut, R. Demadrille and M. Mazzanti, *Dalton Trans.*, 2012, **41,** 1268– 1277; (c) N. Wartenberg, O. Raccurt, E. Bourgeat-Lami, D. Imbert and M. Mazzanti, *Chem. Eur. J.*, 2013, **19,** 3477– 3482 ; (d) S. J. Butler, M. Delbianco, L. Lamarque, B. K. McMahon, E. R. Neil, R. Pal, D. Parker, J. W. Walton and J. M. Zwier, *Dalton Trans.*, 2015, **44,** 4791-4803; (e) M. Delbianco, V. Sadovnikova, E. Bourrier, G. Mathis, L. Lamarque, J. M. Zwier and D. Parker, *Angew. Chem. Int. Ed.* 2014, **53,** 10718 –10722; (f) S. J. Butler, L. Lamarque, R. Pal and D. Parker, *Chem. Sci.*, 2014, **5,** 1750-1756.

13. N. M. Shavaleev, S. V. Eliseeva, R. Scopelliti and J-C. G. Bünzli, *Inorg. Chem.*, 2014, **53,** 5171-5178.

14. S. D. Pietro, D. Imbert and M. Mazzanti, *Chem. Commun.*, 2014, **50,** 10323-10326.

15. S. Kyatskaya, J. R. Galan Mascaros, L. Bogani, F. Hennrich, M. Kappes, W. Wernsdorfer and M. Ruben. *J. Am. Chem. Soc.*, 2009, **131,** 15143–15151.

16. (a) D. Geißler, S. Linden, K. Liermann, K. D. Wegner, L. J. Charbonniere and N. Hildebrandt, *Inorg. Chem.*, 2014, **53,** 1824−1838 ; (b) B. Rogez, H. Yang, E. L. Moal, S. Levé que-Fort, E. Boer-Duchemin, F. Yao, Y-H. Lee, Y. Zhang, K. D. Wegner, N. Hildebrandt, A. Mayne and G. Dujardin, *J. Phys. Chem. C*, 2014, **118,** 18445−18452; (c) F. Morgner, D. Geißler, S. Stufler, N. G. Butlin, H.-G. Löhmannsröben, and N. Hildebrandt, *Angew. Chem. Int. Ed.*, 2010, **49,** 7570–7574.

17. B. Schäfer, C. Rajnák, I. Šalitroš, O. Fuhr, D. Klar, C. Schmitz–Antoniak, E. Weschke, H. Wende and M. Ruben. *Chem. Commun.*, 2013, **49,** 10986–10988.

18. J. Stanley, X. Zhu, X. Yang and B. J. Holliday, *Inorg. Chem.*, 2010, **49,** 2035-2037.

19. (a) J-C. G. Bünzli, A-S. Chauvin, H. K. Kim, E. Deiters and S. V. Eliseeva, *Coord. Chem. Rev.*, 2010, **254,** 2623-2633; (b) M. H. V. Werts, R. T. F. Jukes and J. W. Verhoeven, *Phys. Chem. Chem. Phys*, 2002, **4,** 1542-1548.

20. A. Beeby, I. M. Clarkson, R. S. Dickins, S. Faulkner, D. Parker, L. Royle, A. S. de Sousa, J. A. G. Williams and M. Woods, *J. Chem. Soc., Perkin Trans. 2*, 1999, 493–503.

21. (a) F. W. Lewis, M. J. Hudson and L. M. Harwood, *Synlett.*, 2011, 2609– 2632; (b) Z. Kolarik, *Chem. Rev.* 2008, **108,** 4208– 4252; (c) A. Bremer, C. M. Ruff, D. Girnt, U. Müllich, J. Rothe, P. W. Roesky, P. J. Panak, A. Karpov, T. J. J. Müller, M. A. Denecke and A. Geist, *Inorg. Chem.* 2012, **51,** 5199– 5207.

22. "M86-E01078 APEX2 User Manual", Bruker AXS Inc., Madison, USA, 2006.

23. G. M. Sheldrick, *Acta Cryst.* 1990, **A46,** 467-473.

24. G. M. Sheldrick, *Acta Cryst.* 2008, **A64,** 112-122.

25. Spek, A.L., *J. Appl. Cryst.*, 2003, **36,** 7-13.

26. J. C. de Mello, H. F. Wittmann, R. H. Friend, *Adv. Mater*. 1997, **9**, 230-232.

27. A. S. Chauvin, F. Gumy, D. Imbert, J. C. G.Bünzli, *Spectrosc. Lett.* 2004, **37,** 517- 532.

28. A. S. Chauvin, F. Gumy, D. Imbert, J. C. G.Bünzli, *Spectrosc. Lett.* 2007, **40,** 193- 193.

29. J. P. Byrne, J. A. Kitchen, J. E. O'Brien, R. D. Peacock, T. Gunnlaugsson, *Inorg. Chem.*, 2015, **54 (4),** 1426–1439.